Micro-LEDs and Superluminescent Diodes: Optical Properties and Carrier Dynamics

Ashwin K. Rishinaramangalam, Arman Rashidi, Morteza Monavarian, Andrew A. Aragon, Saadat Mishkat Ul Masabih, and Daniel F. Feezell
University of New Mexico, Albuquerque, NM - 87131

SLD Motivation

Applications of visible SLDs

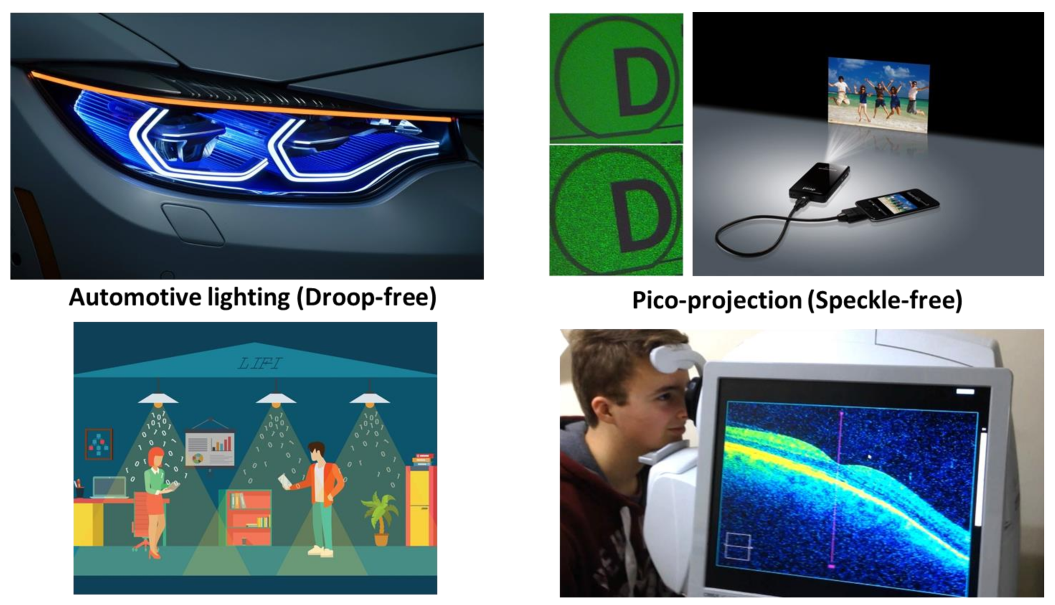

Automotive lighting (Droop-free)

Pico-projection (Speckle-free)

Visible-light Communication (VLC) (High modulation bandwidth)

Optical Coherence Tomography (High resolution imaging)

Advantages of SLDs over LEDs and Lasers

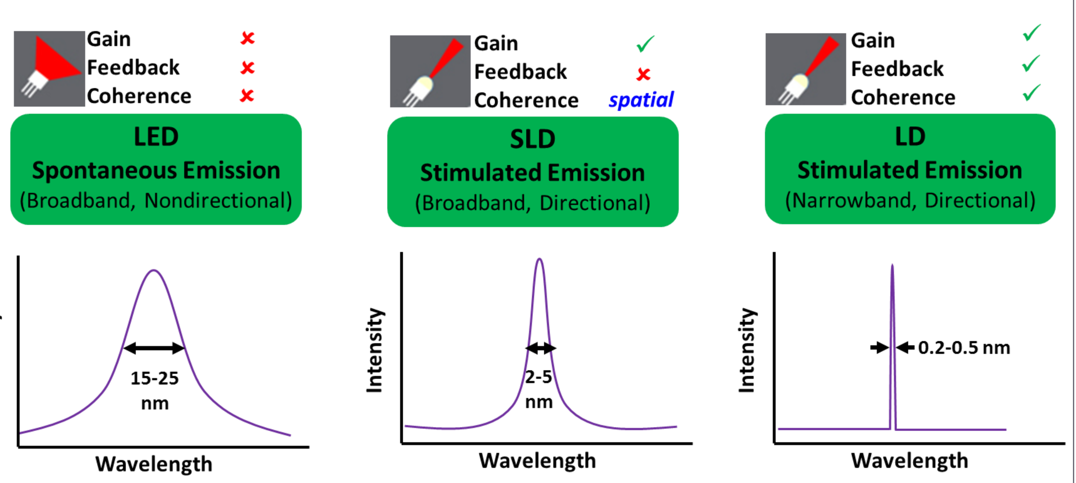

Radiative Efficiency

LED

$$\eta_r = \frac{BN^2}{AN + BN^2 + CN^3}$$

Depends on carrier density → droop

Laser Above Threshold

$$\eta_r = \frac{BN_{th}^2 + R_{st}}{AN_{th} + BN_{th}^2 + CN_{th}^3 + R_{st}}$$

Independent of carrier density → no droop

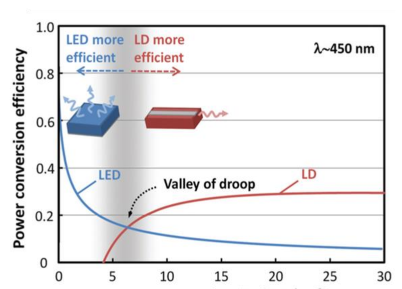

Comparison of the expression for IQE using the ABC model for spontaneous emission dominated devices (LEDs) and stimulated emission dominated devices (SLDs and laser diodes)[J. J. Wierer et al., (2013)]

Advantages of nonpolar SLDs over *c*-plane SLDs

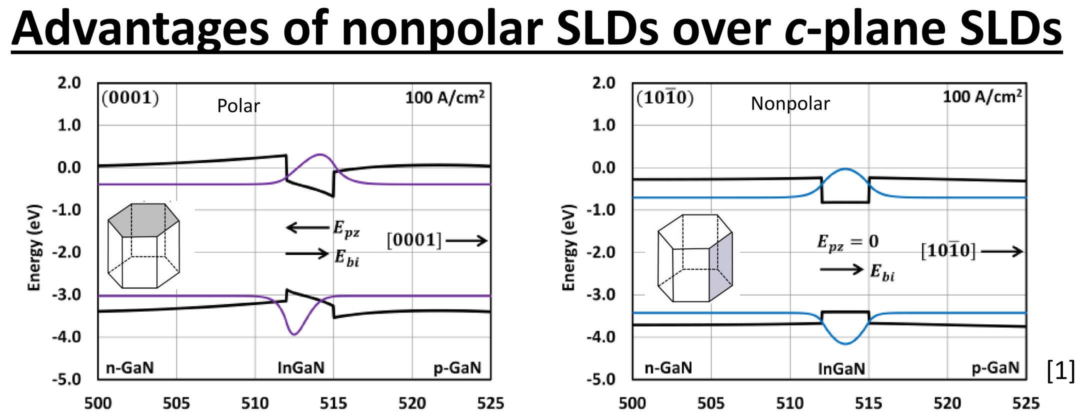

[1]

Energy band simulations of polar and nonpolar active regions at 100 A/cm²

✓ Higher radiative efficiency ✓ Lower blueshift ✓ Shorter carrier lifetime (larger modulation BW)
✓ Allows thicker QWs (higher confinement, lower droop, AlGaN-cladding-free)

Publications

[1] D. Feezell, et al., "Semipolar $(20\bar{2}\bar{1})$ InGaN/GaN Light-Emitting Diodes for High Efficiency Solid-State Lighting," *J. Display Technol.*, vol. 9, pp. 190-198, Feb. 2013.
[2] A. Rashidi, A. Rishinaramangalam, M. Monavarian, S. Mishkat Ul Masabih, A. Aragon, C. Lee, S. DenBaars, and D. Feezell, "Nonpolar GaN-Based Superluminescent Diode with 2.5 GHz Modulation Bandwidth," submitted to *Photon. Technol. Lett.*, Dec. 2019.
[3] A. Rashidi, M. Nami, M. Monavarian, A. Aragon, K. DaVico, F. Ayoub, and D. Feezell, "Differential Carrier Lifetime and Transport Effects in Electrically Injected III-Nitride Light-Emitting Diodes," *Journal of Applied Physics*, vol. 122, pp. 035706(1-9), July 2017.
[4] M. Monavarian, A. Aragon, A. Rashidi, A. Rishinaramangalam, and D. Feezell, "Impact of Crystal Orientation on Modulation Bandwidth of InGaN/GaN Light-Emitting Diodes," *Applied Physics Letters*, vol. 112, pp. 041104(1-4), Jan. 2018.
[5] A. Rashidi, M. Monavarian, A. Aragon, and D. Feezell, "Thermal and efficiency droop in InGaN/GaN light-emitting diodes: decoupling multiphysics effects using temperature-dependent RF measurements," Sci. Reports, vol. 9, pp. 19921, Dec. 2019
[6] A. Rashidi, M. Monavarian, A. Aragon, A. Rishinaramangalam, and D. Feezell, "Nonpolar m-Plane InGaN/GaN Micro-Scale Light-Emitting Diode with 1.5 GHz Modulation Bandwidth," *Electron Device Letters*, vol. 39, pp. 520 – 523, Mar. 2018.
[7] M. Nami, A. Rashidi, M. Monavarian, S. Mishkat-Ul-Masabih, A. K. Rishinaramangalam, S. R. J. Brueck, and D. Feezell, "Electrically Injected GHz-Class GaN/InGaN Core–Shell Nanowire-Based µLEDs: Carrier Dynamics and Nanoscale Homogeneity," *ACS Photonics,* vol. 6, pp. 1618-1625, July 2019.

SLD Epitaxial Growth and Fabrication

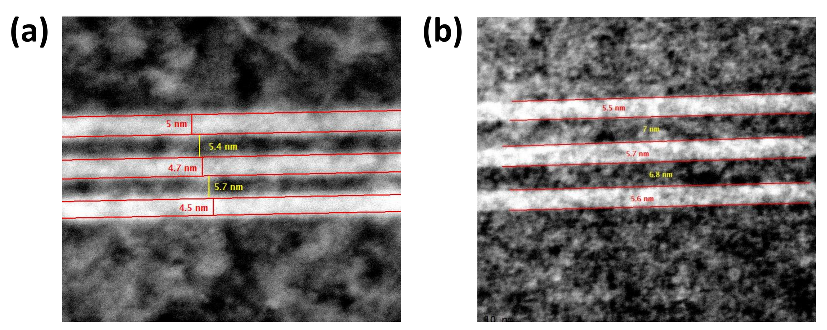

Comparison of active region area of planar *m*-plane LEDs with (a) 3 hr. long p-GaN growth and (b) 45 min long p-GaN growth. The active region quality is improved considerably in the shorter p-GaN growth.

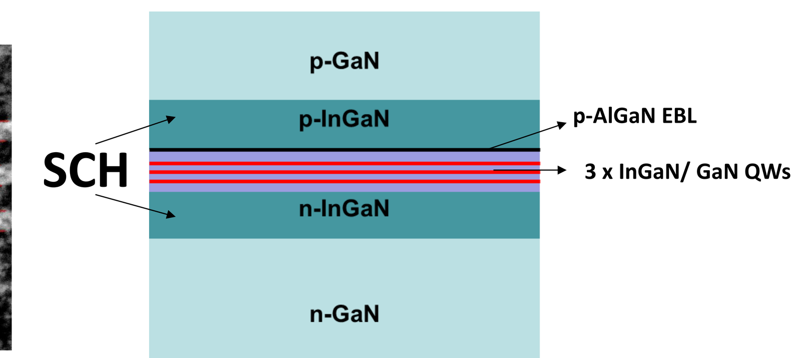

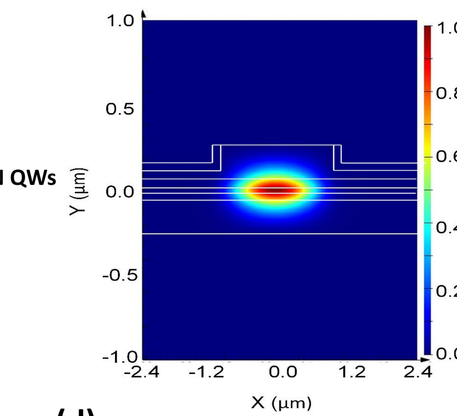

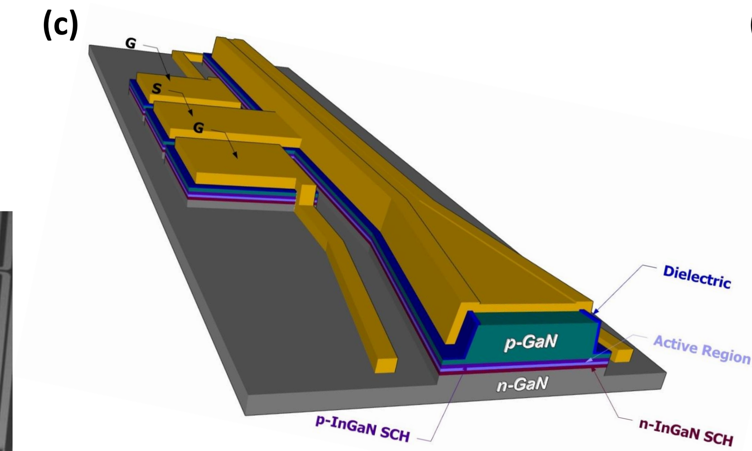

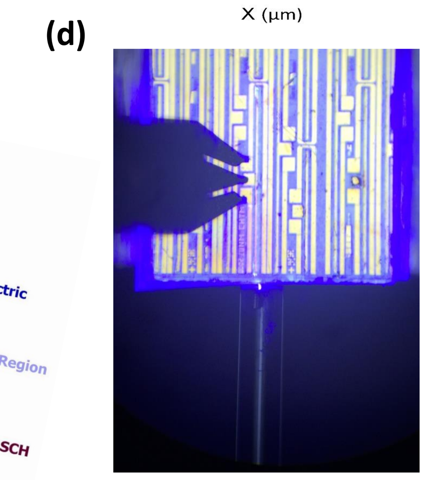

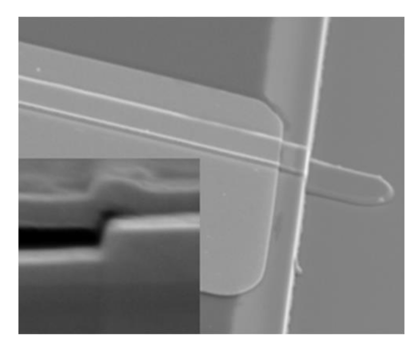

Facet-etch indicating good quality facets. Inset shows cross-section at the ridge

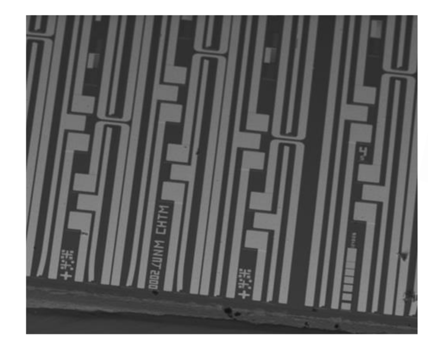

Fabricated SLD and laser arrays with pads for RF testing

(a) Epitaxial layer structure of the SLD indicating the separately-confined heterostructure guiding, whose simulated mode profile using Lumerical (FDTD) is shown in (b). (c) Pictographic illustration of a fabricated tapered waveguide SLD (TSLD). (d) A TSLD under electrical operation.

SLDs Optical and RF Characterization

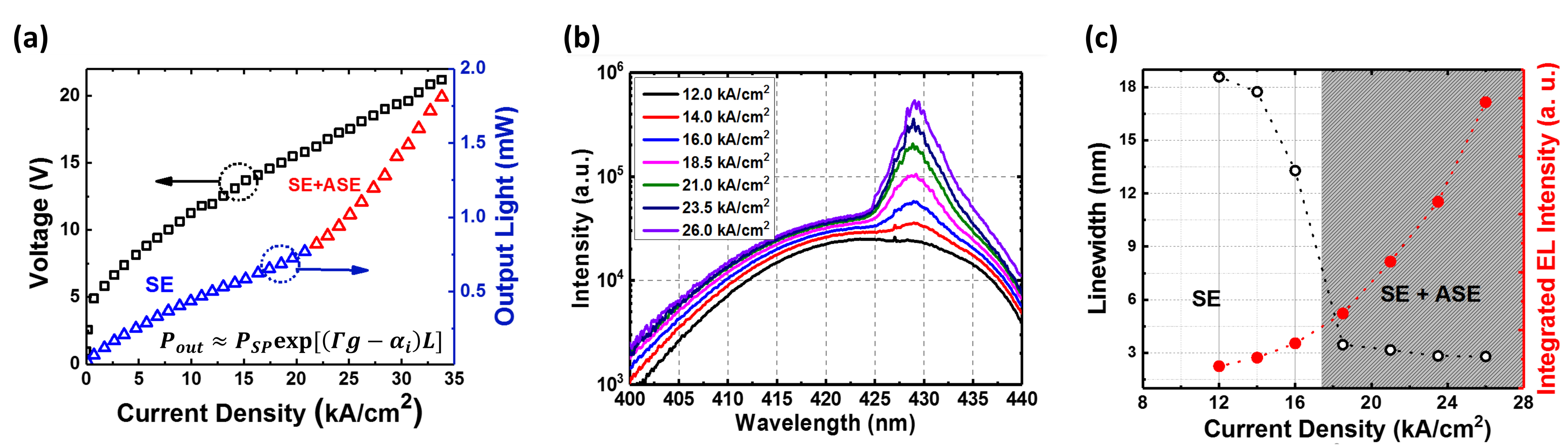

(a) L-J-V characteristics of TSLD. Spectral evolution is shown in (b). (c) Linewidth and total integrated power of the EL spectrum versus current density.

$$f_{3dB} \approx \frac{1.55}{2\pi}\sqrt{\frac{\Gamma^2 v_g^2\, a(\alpha_m+\alpha_i)\beta(J-J_{tr})}{\alpha_m V}}\, exp[\frac{(\Gamma\beta(J-J_{tr})-\alpha_i)L}{2}]$$

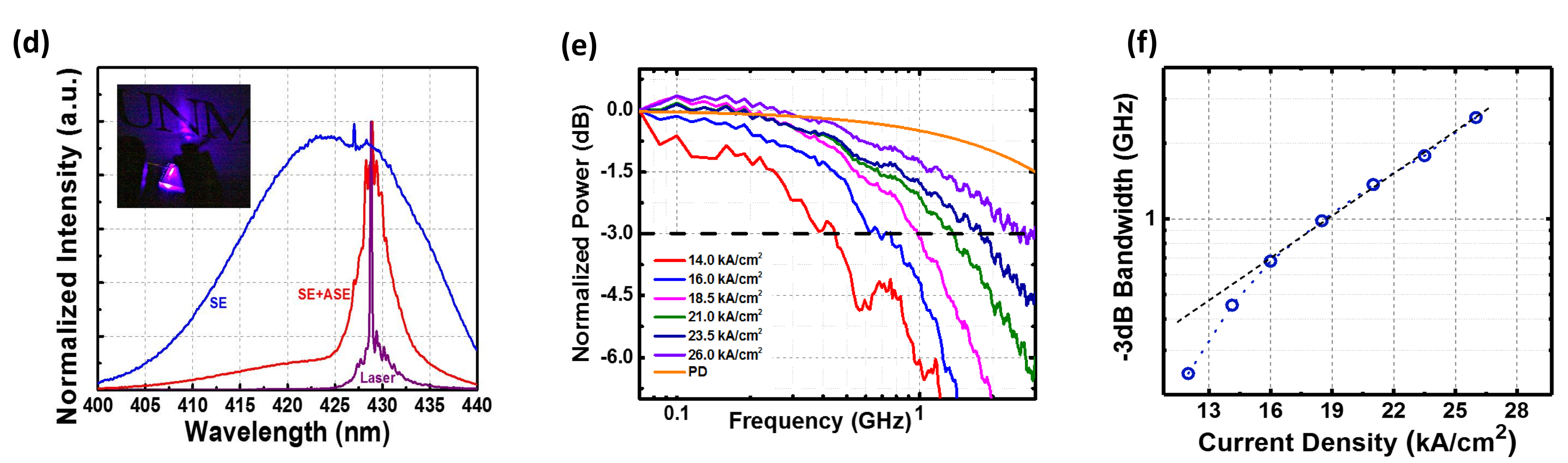

(d) Normalized EL spectra of LED, SLD, and laser on the same chip. (e) Frequency response of the TSLD. The -3 dB RF modulation bandwidth is obtained and plotted versus current density in (f). The log(f_{3dB}) goes linearly as a function of J in the superluminescene regime due to the exponential increase of the o/p power with J, evident from the above equation. [2]

LESA Lighting Enabled Systems & Applications

New Mexico EPSCoR

Carrier Dynamics Measurements

Carrier dynamics model

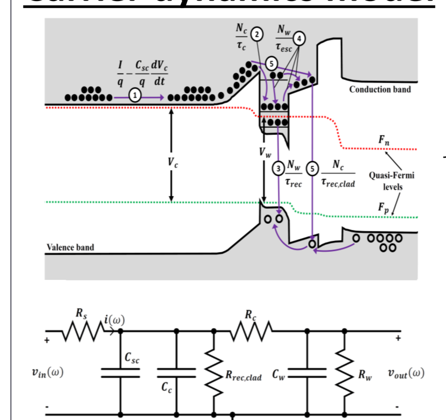

Small-signal rate equations

$$j\omega n_w = -\left[\frac{1}{\tau_{\Delta rec}} + \frac{1}{\tau_{\Delta esc}}\right] n_w + \frac{n_c}{\tau_{\Delta c}}$$

$$j\omega n_c = \frac{i}{q} - j\omega v_c \frac{C_{sc}}{q} + \frac{n_w}{\tau_{\Delta esc}} - \frac{n_c}{\tau_{\Delta c}} - \frac{n_c}{\tau_{\Delta rec,clad}}$$

Input impedance model

$$Z_{in} = R_s + \frac{R_c(1 + j\omega R_w C_w) + R_w}{(1 + j\omega R_w C_w)(1 + j\omega R_c C_{tot}) + j\omega C_{tot} R_w}$$

Associated carrier lifetimes

$$\tau_{rec} = R_w C_w \qquad \tau_{RC} = \frac{R_s}{R_s + R_c}\tau_0$$

$$\tau_{esc} = R_c C_w \qquad \tau_0 = R_c C_{tot}$$

Frequency response model

$$\frac{v_{out}}{v_{in}} = \frac{R_w}{R_s(1 + j\omega\tau_{rec})(1 + j\omega\tau_0) + R_s(j\omega R_w C_{tot}) + R_c(1 + j\omega\tau_{rec}) + R_w}$$

RF measurement station

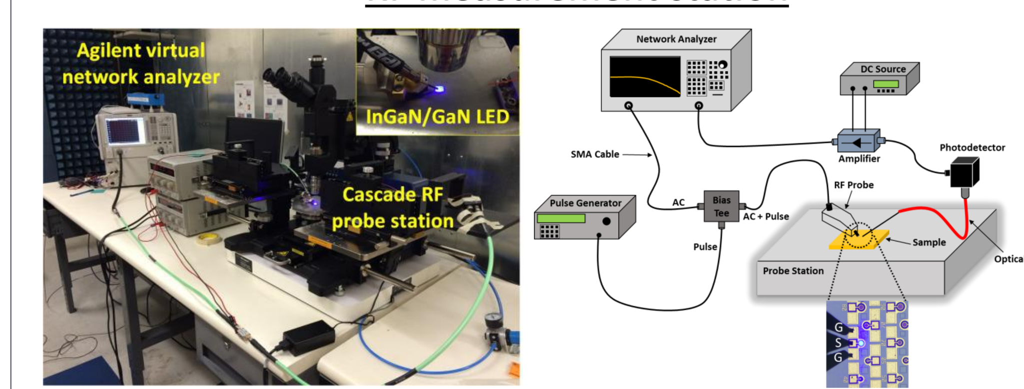

Measured responses with fits

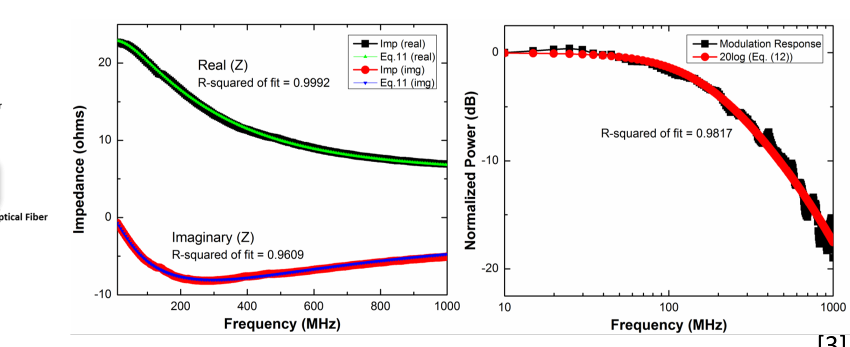

[3]

Micro-LEDs Optical and RF Characterization

Micro-LED structure

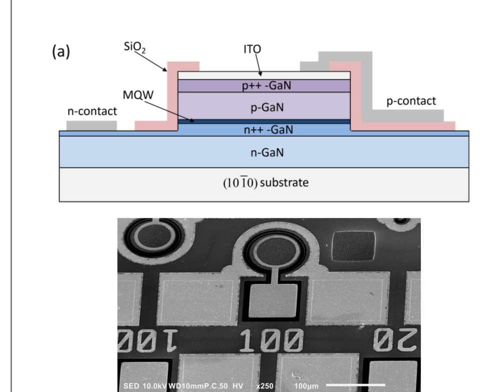

Modulation bandwidth vs. orientation

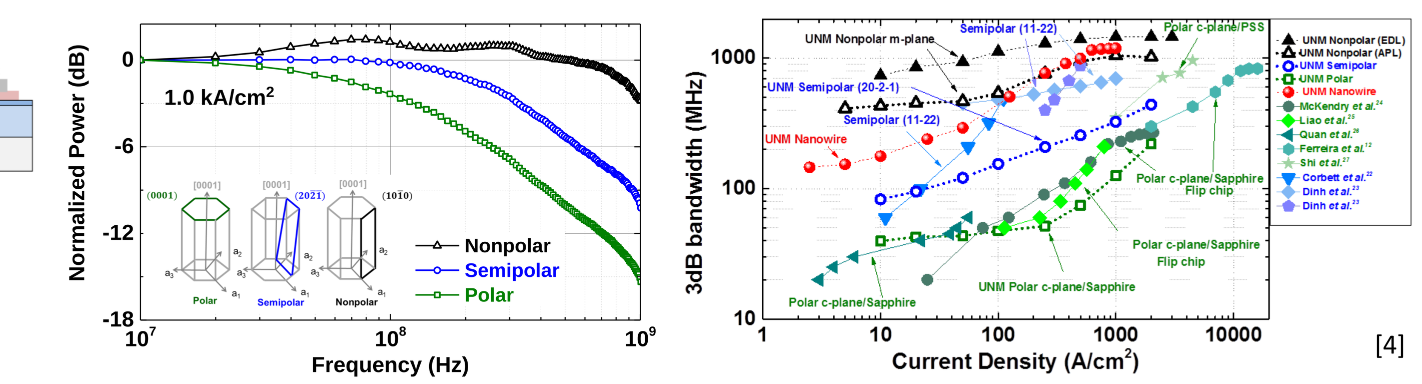

[4]

Temperature-dependent carrier dynamics (radiative and non-radiative rates)

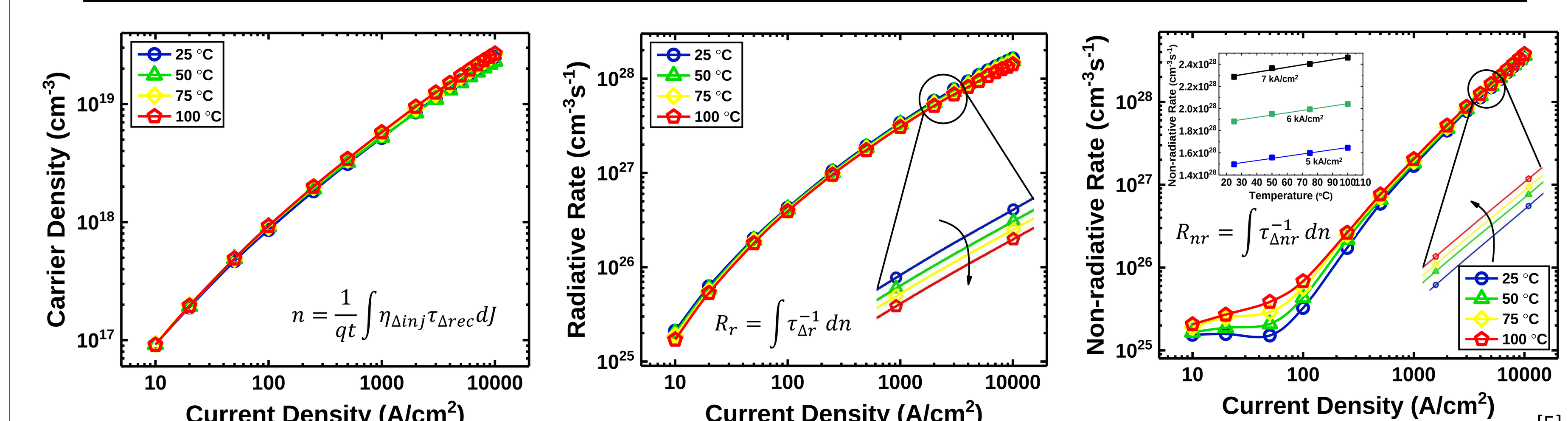

[5]

Nonpolar *m*-plane LEDs with 1.5 GHz bandwidth

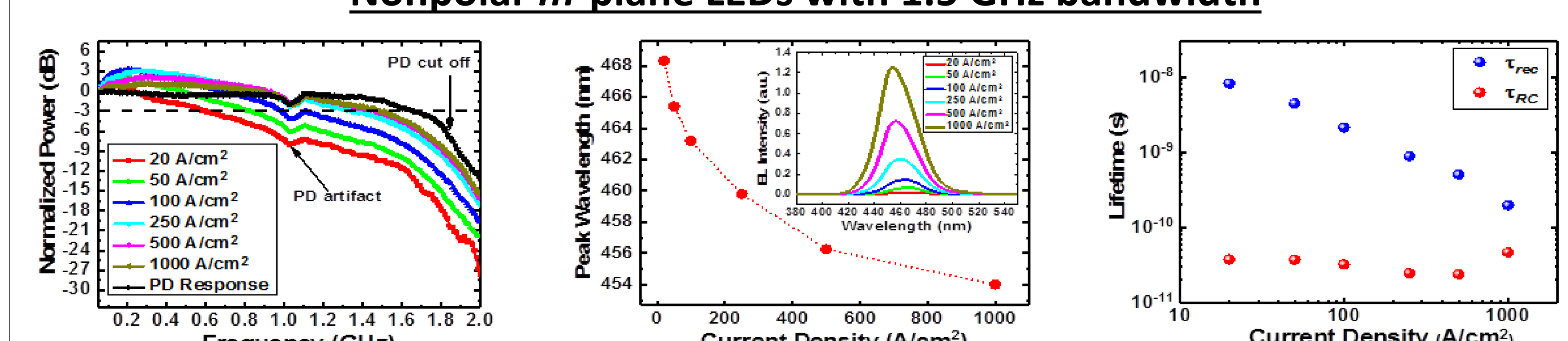

[6]

Core-shell nanowire LEDs with 1.2 GHz bandwidth

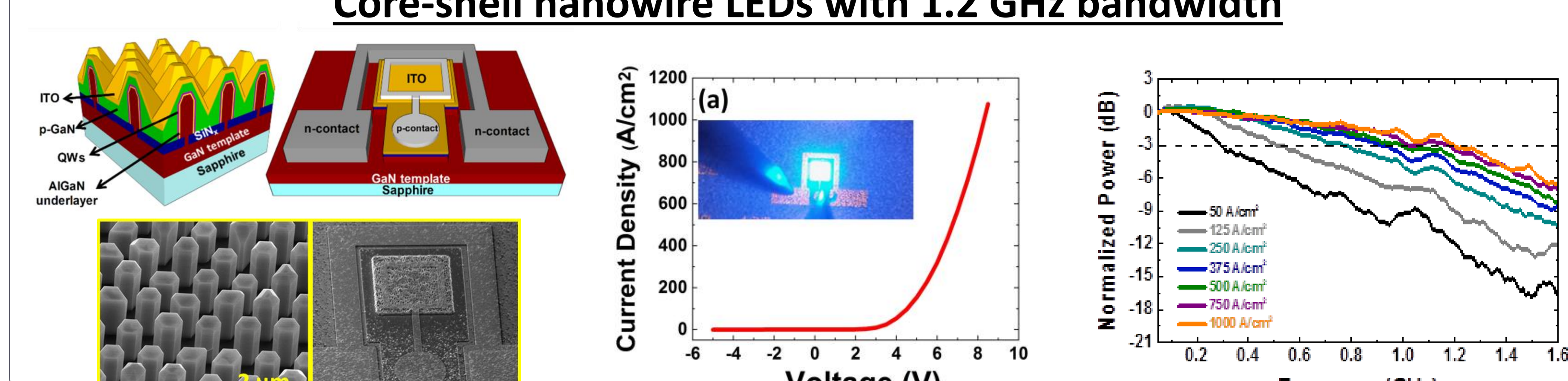

[7]